Science Translational Medicine
AAAS

stm.sciencemag.org/cgi/content/full/11/494/eaau9087/DC1

Supplementary Materials for

Reprogrammed marrow adipocytes contribute to myeloma-induced bone disease

Huan Liu, Jin He, Su Pin Koh, Yuping Zhong, Zhiqiang Liu, Zhiqiang Wang, Yujin Zhang, Zongwei Li, Bjorn T. Tam, Pei Lin, Min Xiao, Ken H. Young, Behrang Amini, Michael W. Starbuck, Hans C. Lee, Nora M. Navone, Richard E. Davis, Qiang Tong, P. Leif Bergsagel, Jian Hou, Qing Yi, Robert Z. Orlowski, Robert F. Gagel, Jing Yang*

*Corresponding author. Email: jiyang@mdanderson.org

Published 29 May 2019, *Sci. Transl. Med.* **11**, eaau9087 (2019)
DOI: 10.1126/scitranslmed.aau9087

The PDF file includes:

Materials and Methods
Fig. S1. Gating/sorting strategy for adipocytes and characterization of primary adipocytes by fluorescent staining.
Fig. S2. Characterization of marrow adipocytes.
Fig. S3. Myeloma-associated adipocytes enhance osteoclastogenesis in vitro.
Fig. S4. Myeloma-associated adipocytes inhibit osteoblastogenesis in vitro.
Fig. S5. Myeloma-associated adipocytes inhibit in vivo extramedullary bone formation.
Fig. S6. Expression of adipokines in myeloma-associated adipocytes.
Fig. S7. Adipokines secreted from myeloma-associated adipocytes enhance osteoclast differentiation.
Fig. S8. Adipokines secreted from myeloma-associated adipocytes suppress osteoblast differentiation.
Fig. S9. Reduced expression of PPARγ in myeloma-associated adipocytes.
Fig. S10. Elevated expression of the PRC2 proteins EZH2 and SUZ12 in myeloma-associated adipocytes.
Fig. S11. Characterization of adipocyte-targeted *Ezh2*-knockout mice.
Fig. S12. Distribution of myeloma cells in the Vk*MYC myeloma cell–bearing mice.
Table S1. Identification of SP1 that binds to the PRC2 complex in adipocytes using mass spectrometry.
Table S2. Characteristics of patients with myeloma and donors with normal BM.
Table S3. Primers used in real-time reverse transcription PCR analysis.
Table S4. Primers used in ChIP-PCR.
References (*33*–*40*)

Other Supplementary Material for this manuscript includes the following:

(available at stm.sciencemag.org/cgi/content/full/11/494/eaau9087/DC1)

Data file S1. Primary data (Excel file).

Materials and Methods

Cell lines and primary myeloma cells. The myeloma cell line ARP-1 was provided by the University of Arkansas for Medical Sciences. Murine myeloma Vk*MYC cell line (Vk12598) (*33*) was provided by the Mayo Clinic. HEK293T and RPMI8226 cells were purchased from the American Type Culture Collection. Primary myeloma cells were isolated from BM aspirates from patients with myeloma using anti-CD138 antibody-coated magnetic beads (Miltenyi Biotec). Myeloma cells were maintained in RPMI 1640 medium with 10% fetal bovine serum (FBS), and HEK293T cells were cultured in Dulbecco's modified Eagle's medium (DMEM) with 10% FBS. All patient samples were obtained from the Myeloma Tissue Bank at The University of Texas MD Anderson Cancer Center, and the related information is listed in table S2. Bone marrow samples were mostly obtained from iliac crest of patients with myeloma following standard procedure for clinical diagnosis, and the residual samples were used for research. Bone lesions in the study participants were characterized by radiologists. This study was approved by the MD Anderson Institutional Review Board.

Antibodies, plasmids, and reagents. The plasmids *HA-SUZ12*, *HA-EZH2*, and *EGFP-SP1* were purchased from Addgene. Except where specified, all chemicals were purchased from Sigma-Aldrich, all antibodies for flow cytometric analysis were purchased from BD Biosciences, all neutralizing antibodies and ELISA kits were purchased from R&D Systems, and all antibodies for Western blot analysis were purchased from Cell Signaling Technology. Calcein acetoxymethyl (Calcein AM) was purchased from Life Technologies. OsteoSense 750 was purchased from PerkinElmer. SiRNAs for the human *SP1* gene and nontarget control siRNA were purchased from Santa Cruz Biotechnology. Tamoxifen was obtained from Sigma-Aldrich and dissolved in corn oil at a concentration of 20 mg/ml as recommended by the manufacturer.

Generation and isolation of adipocytes and collection of adipocyte CM in vitro. Primary mature adipocytes were isolated from aspirates of normal BM or the BM aspirates of patients with myeloma at the time of diagnosis or in remission *(15)*. Briefly, bone marrow aspirates were digested with 0.2 %

collagenase at 37 °C, centrifuged at 700 rpm for 10 minutes, and filtered through 200 μm membrane to separate from hematopoietic and stromal cells. The cells were further washed twice with 1 x PBS. Adipocytes were then stained with LipidTOX Green neutral lipid stain (Molecular Probes, 1:1000) and 5 μg/mL DAPI (Molecular Probes) and sorted by flow cytometry (fig. S1, A to C). First, FSC-A/SSC-A scattered plot were set with log scale and the primary adipocytes were selected as large refractile cells. Next, live cells were gated by inclusion of $DAPI^-$ cells; then the cells with lipid droplets were selected by LipidTOX staining; and finally, singlet cells were selected. An aliquot of the cells was examined by a panel of markers using flow cytometry for the purity of adipocytes. The mature adipocytes displayed high expressions of adipocyte protein 2 (aP2; fatty acid binding protein 4) and BODIPY, but did not express of CD44 and CD105 (MSC and fibroblast markers), CD106 (MSC marker), CD138 (myeloma cell marker), CD24 and Sca-1 (pre-adipocyte markers) *(34)*. Once confirmed, the isolated adipocytes were either used for experiments or incubated in culture with DMEM for 3 days, the supernatants of which were collected as CM. The media that were incubated in an empty well served as controls.
In vitro generation and isolation of human MSCs and adipocytes were performed as described previously *(14)*. The purification and characterization of the mature adipocytes from MSCs are described above. Normal adipocytes were used as controls. Mature adipocytes were maintained in DMEM with 10% FBS. For direct cell-cell contact model, they were seeded onto the back of a Transwell insert (pore size: 0.4 μm) and cultured alone or co-cultured with myeloma cells on the insert for 3 days *(35)*. For non-direct contact model, adipocytes were seeded onto the bottom of culture wells, cultured alone or co-cultured with the myeloma cells on the insert for 3 days. Myeloma cells in the Transwell were removed by a 30-min treatment with 1 mg/ml collagenase, and the adipocytes were cultured for 3 more days. This was followed by a medium change and an additional 3 days of culture, the supernatants of which were collected as CM. In some experiments, the adipocytes were incubated with 5 μM of U0126 (ERK inhibitor) or 10 μM BAY11-7085 (NF- κB inhibitor) for 24 hours. Cells incubated with vehicle served as control. To examine the viability of adipocytes, they were stained with

2 μM calcein AM for 15 min at 37°C in the dark *(36)*, and images were acquired using a fluorescent microscope system (Zeiss Axiovert 200M inverted microscope and AxioCam MRc5 digital camera) with a fluorescein isothiocyanate filter at 10x magnification. Images of unstained adipocytes served as control. Adipocytes were also fixed in 4% paraformaldehyde, stained with Oil Red O for 1 h, and observed under a light microscope.

In vitro osteoblast and osteoclast formation and function assays. MSCs were obtained from the BM of healthy donors, and mature osteoblasts were generated from MSCs with osteoblast medium as described previously *(4)*. The maturity of the osteoblasts was determined by measuring their ALP activity using ALP assays, and the bone formation activity of osteoblasts was determined using Alizarin red S (Sigma-Aldrich) staining as described previously *(4)*.

Human monocytes were isolated from peripheral blood mononuclear cells of health donors (Gulf Coast Regional Blood Center) and cultured as described previously *(4)* to obtain the precursors of osteoclasts. The precursors derived from human monocytes were used. These cells were cultured in M-CSF (25 ng/ml) with or without a low dose of RANKL (10 ng/ml) or adipocyte CM for 7 days to induce mature osteoclast formation. TRAP staining for the detection of mature osteoclasts was performed using a leukocyte acid phosphatase kit (Sigma-Aldrich) according to the manufacturer's instructions. Quantitative measurement of active TRAP isoform 5b was done using a BoneTRAP assay (Immunodiagnostic Systems) according to the manufacturer's instructions.

Western blot analysis. Cells were harvested and lysed with 1 × lysis buffer (Cell Signaling Technology). Cell lysates were subjected to SDS-PAGE, transferred to a polyvinylidene difluoride (PVDF) membrane, and immunoblotted with antibodies against PPARγ, EZH2, integrin α6, SUZ12, SP1, H3K27me3, H3, HA, EGFP, phosphorylated and non-phorphorylated ERK1/2, JNK, p38 MAPK, IκBα, Akt, and β-actin (Cell Signaling Technology).

Quantitative real-time PCR. Total RNA was isolated using an RNeasy kit (QIAGEN). An aliquot of 1 μg of total RNA was subjected to reverse transcription (RT) with a SuperScript II RT-PCR kit (Invitrogen) according to the manufacturer's instructions. Quantitative PCR was performed using SYBR Green Master Mix (Life Technologies) with the QuantStudio 3 Real-Time PCR System (Life Technologies). The primers used are listed in table S3.

SiRNA transfection and luciferase assay in vitro. Adipocytes were transfected with 50 nM siRNA targeted against human *SP1* using Lipofectamine 2000 (Life Technologies). A scrambled siRNA served as a control. Cells were examined 48 h after transfection. The construct covers the full-length (Luc-*PPARγ*: -1 kb to 500 bp,), two truncated forms (Luc-*PPARγ*-Δ1: -500 bp to 500 bp; Luc-*PPARγ*-Δ2: -100 bp to 500 bp), and a mutated form (Luc-*PPARγ*-mut: GGGCGG to GATAAG) made around -178 bp upstream of the starting codon in the promoter of the *PPARγ* gene were subcloned into the pGL2 vector, and their transcriptional activities in HEK293T cells were examined using a Dual-Luciferase Reporter Assay System (Promega) according to the manufacturer's instructions. The luciferase activity of *Luc-PPARγ* constructs was set at 1. The primers used in the subcloning are listed below.

	Forward	Reverse
PPARγ	CATCTCGAGTGTACCAGAGGGG CAATAACCACA	CAGAAGCTTGCTGTCCTGGAA GCCGGG
PPARγ-Δ1	CATCTCGAGGAGAAAACCAAGG GACCCGAAA	CAGAAGCTTGCTGTCCTGGAA GCCGGG
PPARγ-Δ2	TTAATAGATCTCCCCACCCCCAC CCCCA	CAGAAGCTTGCTGTCCTGGAA GCCGGG
PPARγ-mut	CCCGGGCTCGGCCGCTTATCGC GCACAGTAGGGC	GCCCTACTGTGCGCGATAAGC GGCCGAGCCCGGG

Cell proliferation assays, flow cytometry, and ELISA. The proliferation of adipocytes was assessed using a CellTiter 96 AQueous One Solution Cell Proliferation Assay (Promega) following the manufacturer's instructions. The cells were fixed and stained with BODIPY or with the antibodies against CD138, CD19, CD56, CD24, CD44, CD105, CD106 or Sca-1. For aP2 staining, fixed adipocytes were permeabilized and blocked in 1% BSA in 1 x PBST for 30 min at 37°C. Then the cells were incubated with aP2 antibody (LifeSpan BioSciences Inc) and subsequent secondary antibodies conjugated with Alexa Fluor 488 (Invitrogen) or goat IgG isotype control (Novus Biologicals), and measured by a BD LSRFortessa flow cytometer (BD Biosciences). The results were analyzed using Flow Jo software. In addition, the concentrations of adipokines in CM were measured using an ELISA kit (R&D Systems) according to the manufacturer's instructions.

Fluorescent staining. Adipocytes were fixed in 4% paraformaldehyde and stained with single or in combinations of the following dyes: 1.5 µg/mL LipidTOX Green (Molecular Probes) for neutral lipid, CellMask^{TM} Orange Plasma (Molecular Probes, 1:1000) for membrane, and 5 µg/mL DAPI for nuclei. To observe the cells, adipocytes were resuspended in 80% glycerol and mounted onto a glass slide. Immunofluorescence images were acquired using a Leica SP8 confocal microscope.

Immunohistochemistry. Formalin-fixed, paraffin-embedded sections of BM biopsy samples obtained from patients with myeloma were deparaffinized and stained as described previously *(37)*. Slides were stained with anti-perilipin (Cell Signaling Technology) or anti-CD138 (LifeSpan BioSciences) antibodies using an EnVision System (DAKO) following the manufacturer's instructions and counterstained with hematoxylin. Subcutaneous tissue samples extracted from mice were fixed, sectioned, and processed similarly.

Immunoprecipitation and pull down assays. Cells were lysed and incubated on ice for 15 min. The total protein lysate (500 mg) was immunoprecipitated with an agarose-immobilized antibody at 4°C overnight. After washing six times, the beads were spun down and resuspended in 30 µl of 1× SDS buffer. After boiling for 5 min, pull-down samples were run on a SDS-PAGE gel along with a 5% input

sample and transferred to a PVDF membrane for immunoblotting. IgG was used as a control and total cell lysates were used as input controls. For the pull down assay, HEK293T cells were transfected with either *HA-EZH2* or *HA-SUZ12* plasmid. Lysates of the cells pulled down with HA beads were further incubated with cell lysates transfected with *EGFP-SP1*. The immunoprecipitates and whole cell lysates (WCL) were immunoblotted. Cells not transfected with *HA-EZH2* or *HA-SUZ12* plasmid or WCL served as controls.

ChIP and ChIP-seq assays. Cells were fixed in 4% formaldehyde and sonicated to prepare chromatin fragments. Chromatin samples were immunoprecipitated with antibodies against SUZ12, EZH2, H3K27me3, SP1, and control immunoglobulin G (IgG) at 4°C for 3 h. Immunoprecipitates and total chromatin inputs were reverse cross-linked; DNA was isolated and analyzed using PCR with primers targeting four regions of the promoter regions of *PPARγ* (Fig. 4D). The primer sequences used are listed in table S4. The ChIP-PCR products were separated via gel electrophoresis and quantified using the Image J software program (National Institutes of Health). Relative fold enrichment was calculated by determining the immunoprecipitation efficiency (ratio of the amount of immunoprecipitated DNA to that of the input sample, IgG control group set to 1).

Fifteen to 25 ng of ChIP DNA immunoprecipitated with anti-H3K27me3 antibodies or control IgG from parallel experiments was used for library preparation and sequencing using an Ion Proton system (ThermoFisher). The raw sequencing reads obtained were mapped to a human reference genome. ChIP–seq peaks were called using MACS and NGS Analyzer (Genomatix).

DNA microarray analysis. DNA microarray analysis was performed as described previously *(38)*. Specifically, the gene expressions in adipocytes isolated from BM aspirates of healthy donors and those from patients in remission were compared. A greater than twofold difference in expression was deemed significant. The expression of those genes was further examined using quantitative PCR.

Mass spectrometry. Immunoprecipitates of adipocytes with *HA-EZH2* against an anti-HA antibody were subjected to a SDS-PAGE gel. Gel bands stained with Coomassie blue were excised separately,

alkylated, and digested with trypsin. The tryptic peptides were then analyzed using a nano-LC/MS/MS (Thermo Fisher Scientific) coupled with an 1100 HPLC (Agilent Technologies). The MS/MS spectra were searched using the SEQUEST software program with the BioWorks Browser (version 3.3.1; Thermo Fisher Scientific) against the NCBI database. Adipocytes transfected with an empty vector served as controls.

In vivo mouse experiments, measurement of tumor burden, radiography, μ-CT, and bone histomorphometry. NOD-*scid* IL2Rg^{null} (NSG), C57BL/6, homozygous *Ezh2*$^{flox/flox}$, and Adipoq-CreER mice were purchased from The Jackson Laboratory and maintained in American Association of Laboratory Animal Science-accredited facilities. All in vivo mouse studies were approved by the MD Anderson Institutional Animal Care and Use Committee (#00000418-RN02).

To monitor the tumor burden, serum samples were collected from the mice weekly and tested for the presence of myeloma-secreted M proteins or light chains using ELISA and spectrophotometric analysis. To examine the lytic bone lesions, radiographs were scanned with a Bruker In-Vivo Xtreme imaging system. μ-CT was conducted with the Scanco μCT-40 system (55-peak kilovoltage and 145-μA x-ray source). Mouse femurs were scanned at 16-μm resolutions and calvarial samples were scanned at 30-μm resolutions, and further analyzed with Scanco (Scanco Medical) or Microview (Parallax Innovations) software. Bone tissues were fixed in 10% neutral-buffered formalin and decalcified, and sections of them were stained with toluidine blue or TRAP following standard protocols. Both analyses were done using the BIOQUANT OSTEO (v18.2.6) software program (BIOQUANT Image Analysis Corporation).

Examination of lytic lesions in SCID-hu mouse models. SCID-hu hosts were established as reported previously *(4)*. Human fetal bone chips (Advanced Bioscience Resources, Inc) were implanted subcutaneously into the right flanks of NSG mice. An aliquot of 50 μl of CM collected from adipocytes isolated from BM aspirates from patients with myeloma or adipocytes treated with myeloma cells were injected directly into the implanted bone chips. Control SCID-hu mice did not receive CM or received

CM from adipocytes isolated from BM aspirates from healthy donors or normal adipocytes that were untreated or treated with normal plasma cells. The injections were done three times a week for 16 weeks, and the bone lesions were monitored using radiographic imaging. At the end of experiment, the bone chips were fixed and processed for bone histomorphometric analysis.

In vivo extramedullary bone formation. In vivo extramedullary bone formation in NSG mice was established and examined using a method based on that in a previous study *(18)*. Briefly, a mixture of 2 × 10^6 human BM-derived MSCs, 2 × 10^6 human endothelial colony-forming cells, and 2 × 10^6 adipocytes that were either untreated or treated with myeloma cells in 0.2 ml of Matrigel was subcutaneously injected into the left or right flanks of mice, respectively. At 6-8 weeks after inoculation, mice were intravenously injected with OsteoSense 750, a fluorescent-tagged bisphosphonate dye that targets hydroxylapatite to assess osteoid. The next day, mice were imaged using an IVIS Spectrum in vivo imaging system (PerkinElmer) according to the manufacturer's recommendations. Subcutaneous tissues then extracted from the mice, fixed in 4% paraformaldehyde and embedded in paraffin. The sections were stained with H&E. The paraffin section was subjected to immunohistochemical staining.

Calvarial bone formation model. A calvarial defect that was around 2 mm diameter were established in NSG mice modified from the previous protocol *(39)*. A mixture of hydrogel (20 µl, Sigma Aldrich) and 1 × 10^6 of normal adipocytes or the adipocytes pre-exposed to myeloma cells ARP-1 or RPMI8226 were transplanted onto the site of calvarial defect. Implantation of hydrogel alone served as controls. Two weeks later, mice were euthanized and mouse calvaria were fixed with 10% formalin for 3 days and then assessed with a Scanco µ-CT scanner.

Generation of Cre-expressing *Ezh2*-knockout mice and establishment of a complete remission mouse model of myeloma. The mice used for the generation of inducible adipose-specific *Ezh2*-knockout mice were both purchased from Jackson Laboratories. *Ezh2*$^{flox/flox}$ mice were crossed with transgenic mice expressing tamoxifen-inducible Cre recombinase under the control of the *Adiponectin* promoter. Progeny with Cre expression (*Adipoq*-CreER-*Ezh2*$^{flox/+}$) were back-crossed with *Ezh2*$^{flox/flox}$

mice to generate inducible adipose-specific *Ezh2*$^{flox/flox}$ knockout mice. The primers used for genotyping were *Ezh2*/forward (5'-CATGTGCAGCTTTCTGTTCA-3'), *Ezh2*/reverse (5'-CACAGCCTTTCTGCTCACTG-3'), *Cre*/forward (5'-ATTGCTGTCACTTGGTCGTGGC-3'), and *Cre*/reverse (5'-GGAAAA TGCTTCTGTCCGTTTGC-3'). Mice (*Adipoq-CreER-Ezh2*$^{flox/flox}$) were given 75 mg/kg tamoxifen or corn oil intraperitoneally daily for 5 consecutive days to generate mice with deletion of the *Ezh2* gene in adipocytes or control mice *(40)*. Also, Western blotting was conducted to confirm ablation of Ezh2 expression in the BM of randomly selected mice.

To establish the complete remission mouse model, Vk*MYC murine myeloma cells were used and maintained based on methods described in previous studies *(33)*. Briefly, the cells were maintained in C57BL6 mice and sorted as murine CD138^{+} cells from mouse spleens. Purified Vk*MYC cells (1×10^{6}/mouse) were injected intrafemorally into control and *Ezh2*-knockout mice. At week 4, 1 mg/kg bortezomib and 2 mg/kg melphalan were given intraperitoneally to the mice three times a week for 2 weeks. Serum M proteins were measured using ELISA to evaluate the tumor burden. Starting at week 6, the mice were myeloma-free according to serum M proteins and percentages of CD138^{+} cells in BM aspirates from randomly selected mouse femurs. From week 6 to week 8, mice with no evidence of myeloma were defined as being in complete remission. Untreated and uninjected mice served as healthy controls. Radiography was used to evaluate bone lesions. At week 8, the mice were euthanized, and their femurs were obtained for bone histomorphometric analysis. Also, the relative expression for *Ezh2*, *Suz12*, *Pparγ*, and adipokines in the BM were evaluated.

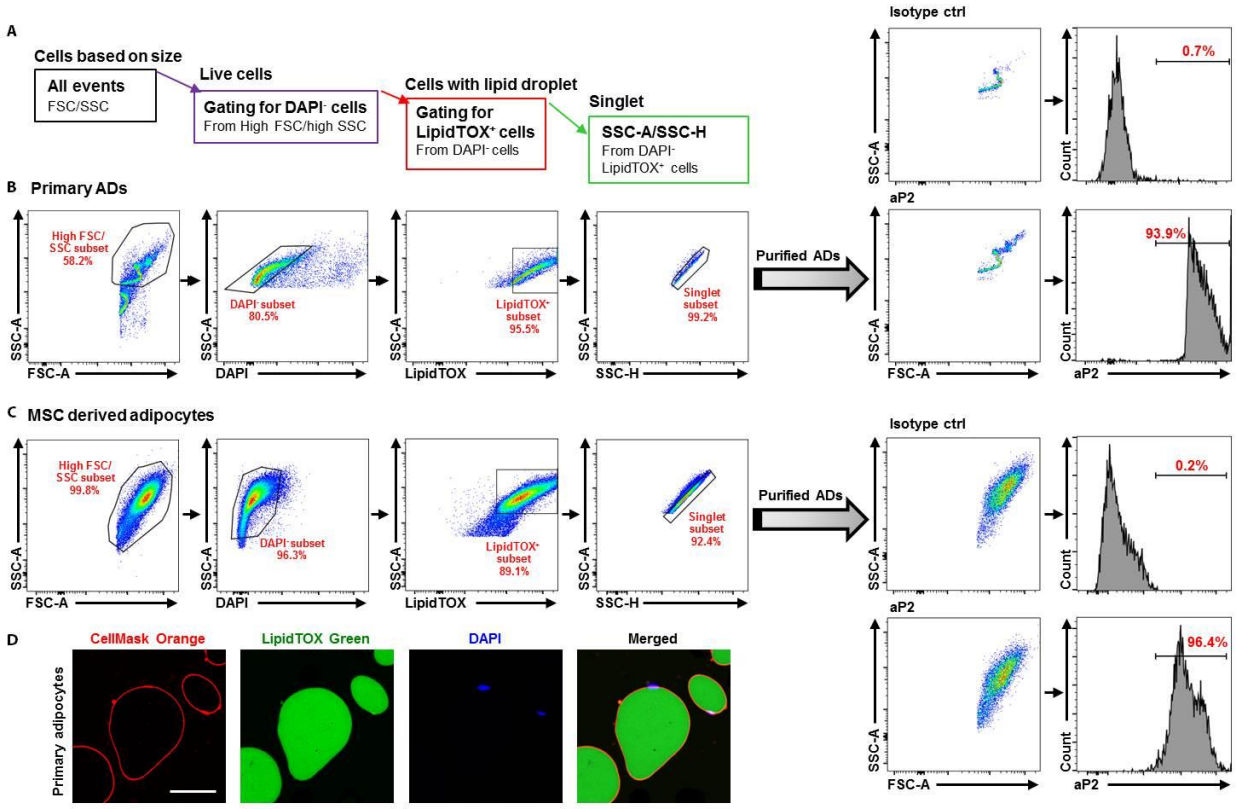

Fig. S1. Gating/sorting strategy for adipocytes and characterization of primary adipocytes by fluorescent staining. (**A**) Gating/sorting strategy for purification of primary adipocytes is diagrammed at the top. Cells were stained with 5 µg/mL DAPI and 1.5 µg/mL LipidTOX and sorted as following: first, using the FSC versus SSC plot, primary adipocytes are gated by their large size and refractile property. Then, the population that excludes DAPI as live cells are selected; of those, cells that are positively stained with LipidTOX are selected; finally, only singlet cells are selected by SSC peak height versus peak area plot. (**B-C**) Representative plots for the purification of primary adipocytes (**B**) and MSC derived adipocytes (**C**) by sorting. An aliquot of fixed purified adipocytes (ADs) were further examined by flow cytometry after staining with an anti-aP2 antibodies or isotype controls. (**D**) Representative images of primary adipocytes labeled with CellMask Orange (1:1000 dilution), 5 µg/mL DAPI, and 1.5 µg/ mL LipidTOX. The cells were fixed, stained, and examined under a confocal microscope. Representative results of at least three experiments are shown.

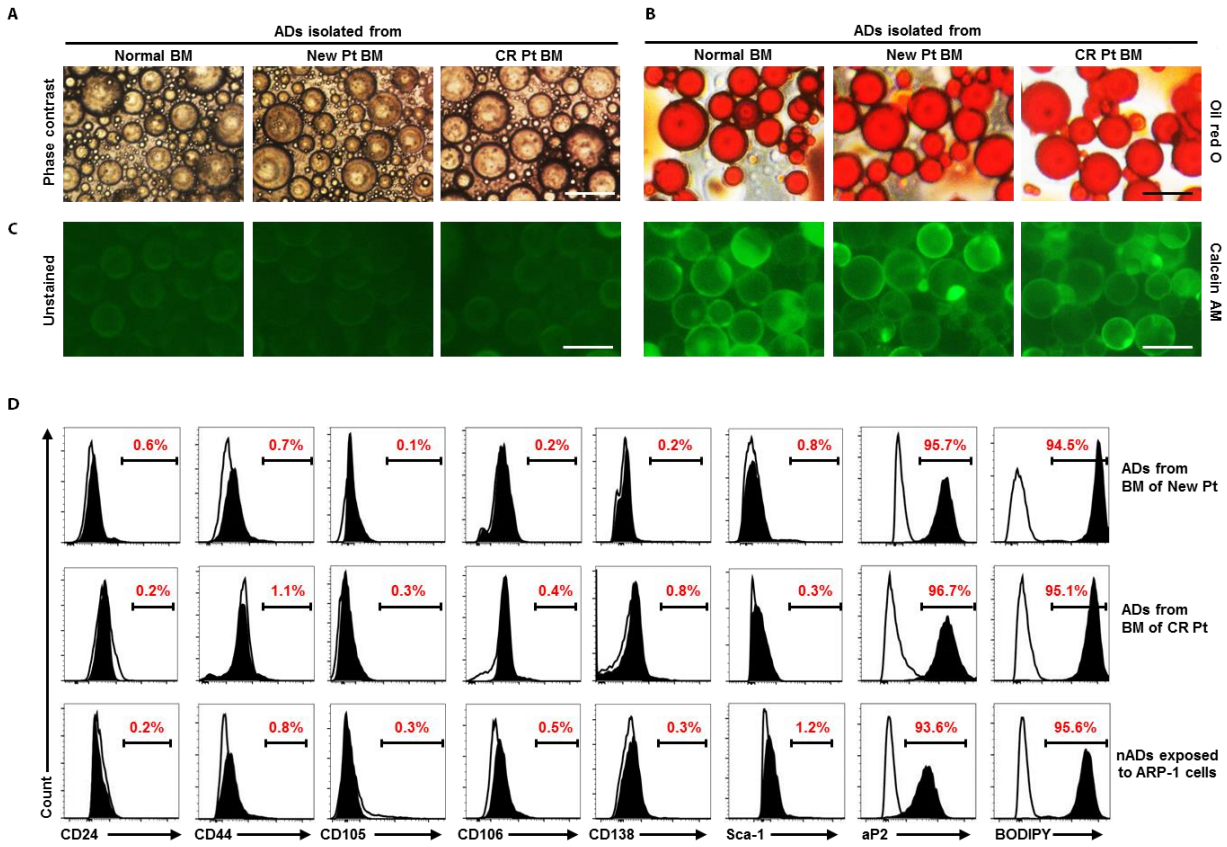

Fig. S2. Characterization of marrow adipocytes. Adipocytes were isolated from aspirates from normal BM (Normal), BM of patients with newly diagnosed myeloma (New Pt) and patients with myeloma in complete remission (CR Pt). (**A-C)** Adipocytes are shown under a phase-contrast microscope (**A**), stained with Oil Red O for the lipid droplets of mature adipocytes (**B**), and stained with calcein AM or unstained (control) for cell viability of adipocytes (**C**). Scale bars, 100 μm. (**D**) Identification of the cell population of mature adipocytes by flow cytometry. Shown are representative histograms of CD24, CD44, CD105, CD106, CD138, Sca-1, aP2, and BODIPY in the adipocytes isolated from BM of one patient with newly diagnosed myeloma (New Pt) and one patient in complete remission (CR Pt) or in normal adipocytes (nADs) exposed to myeloma ARP-1 cells. Open histograms indicate isotype controls. Representative results of three experiments are shown.

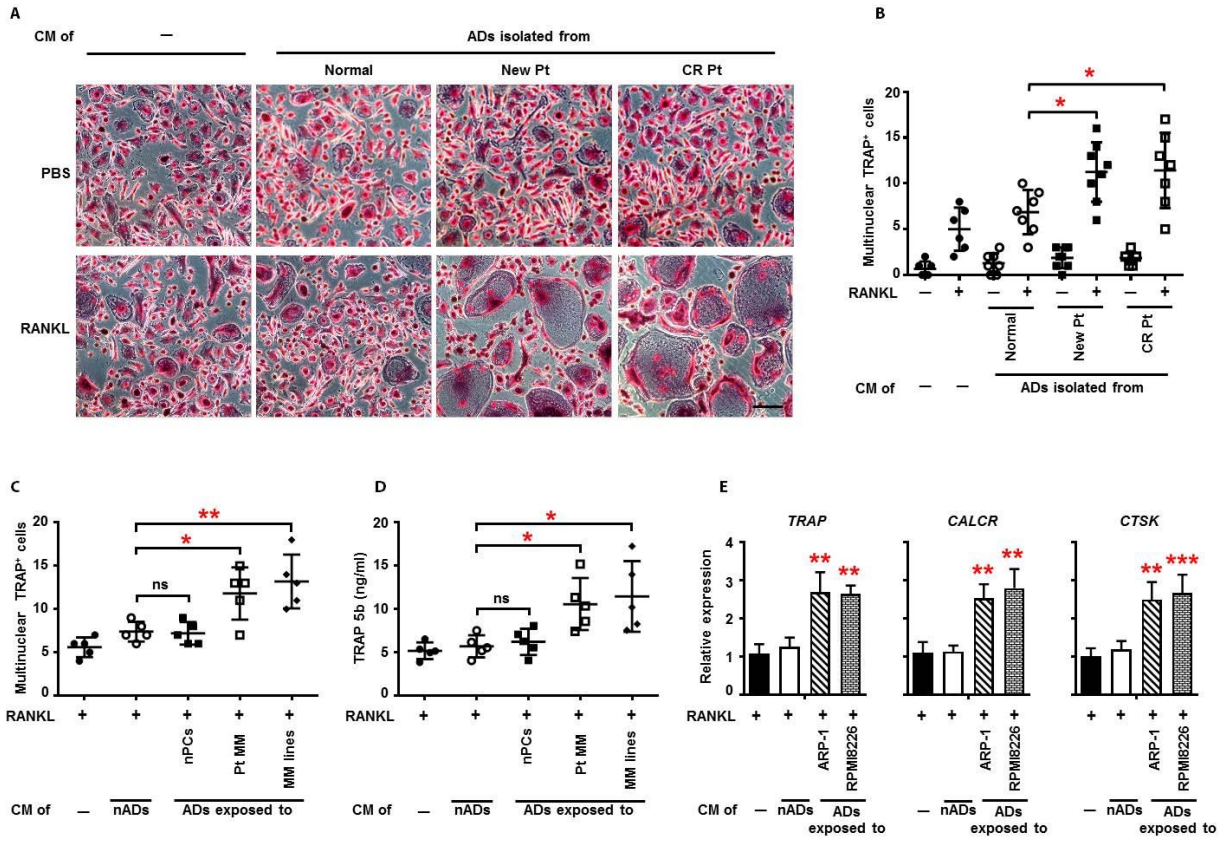

Fig. S3. Myeloma-associated adipocytes enhance osteoclastogenesis in vitro. Precursors of osteoclasts were cultured in M-CSF (25 ng/ml) with RANKL (10 ng/ml) or PBS in the presence of CM from adipocytes (ADs) isolated from normal BM (Normal; *n* = 7), BM aspirates from patients with newly diagnosed myeloma (New Pt; *n* = 8), or BM aspirates from patients with myeloma in complete remission (CR Pt; *n* = 7) or CM from normal adipocytes (nADs) or adipocytes exposed to normal plasma cells (nPCs; *n* = 5), patient-derived myeloma cells (Pt MM; *n* = 5), or myeloma cell lines (MM lines: ARP-1, RPMI 8226, U266, MM.1S, and CAG). Addition of PBS or no addition of CM of adipocytes served as a control. Shown are the morphologies (**A**) and numbers (**B** and **C**) of multinuclear (⩾3) TRAP^{+} cells, TRAP 5b (**D**), and relative expression of the *TRAP*, *CALCR*, and *CTSK* genes in precursors of osteoclasts (**E**). Scale bars, 100 μm. Data are averages ± SD. Each experiment was repeated three times. **P* < 0.05; ***P* < 0.01; ****P* < 0.001. ns, not significant. All *P* values were determined using one way ANOVA.

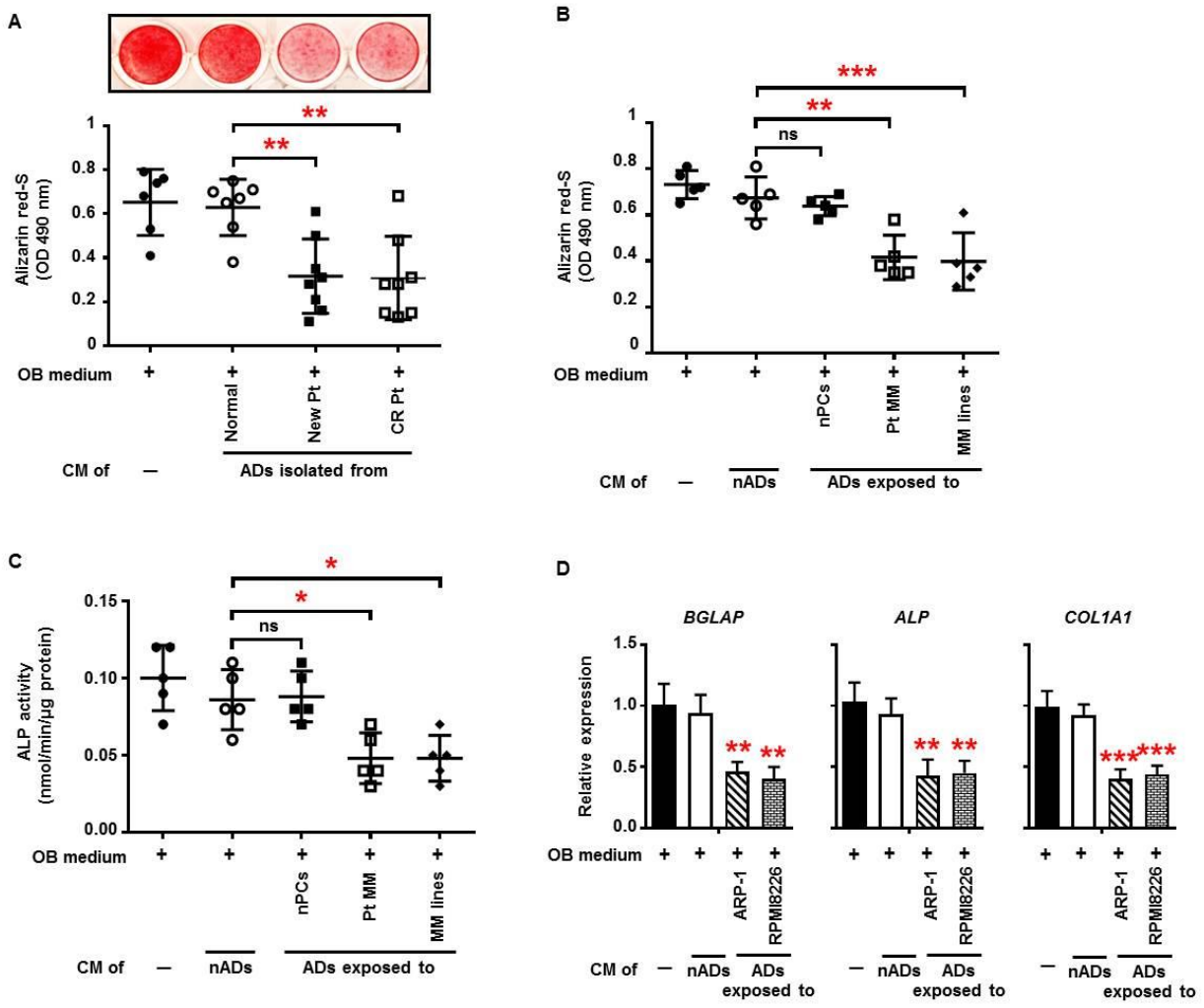

Fig. S4. Myeloma-associated adipocytes inhibit osteoblastogenesis in vitro. MSCs were cultured in osteoblast (OB) medium with addition of CM from adipocytes (ADs) isolated from normal BM (Normal; *n* = 7), BM aspirates from patients with newly diagnosed myeloma (New Pt; *n* = 8), or BM aspirates from patients with myeloma in complete remission (CR Pt; *n* = 8) or adipocytes exposed to normal plasma cells (nPCs; *n* = 5), patient-derived myeloma cells (Pt MM; *n* = 5), or myeloma cell lines (MM lines: ARP-1, RPMI 8226, U266, MM.1S, and CAG). Without CM served as controls. Shown are representative images (**A**) and summarized data of Alizarin red S staining (**B**), ALP activity (**C**), and the relative expression of *BGLAP*, *ALP*, and *COL1A1* genes in MSCs (**D**). Data are averages ± SD. Each experiment was repeated three times. ns, not significant; **P* < 0.05; ***P* < 0.01; ****P* < 0.001. All *P* values were determined using one way ANOVA.

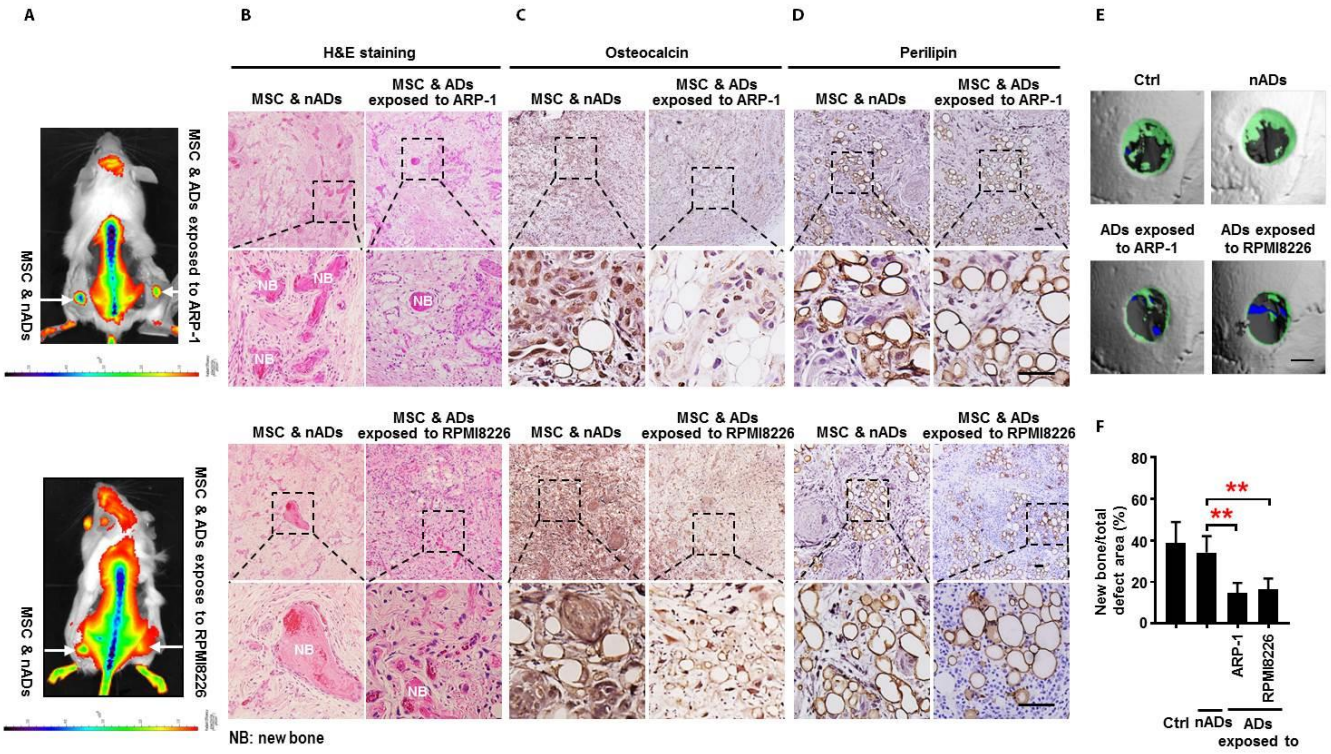

Fig. S5. Myeloma-associated adipocytes inhibit in vivo extramedullary bone formation. (**A-C)** MSCs combined with normal adipocytes (nADs) or adipocytes (ADs) exposed to the myeloma cell line ARP-1 or RPMI8226 were mixed with Matrigel, and the mixture was subcutaneously implanted in NSG mice. 8 weeks after implantation the mice were intraperitoneally injected with OsteoSense 750 to assess new bone formation in the tissues. The subcutaneous tissues were collected postmortem and subjected to hematoxylin and eosin (H&E) staining or immunohistochemical staining for an antibody against osteocalcin (a marker of mature osteoblasts). Shown are representative images of the bone density in mice (**A**) and H&E (**B**) and immunohistochemical stains with antibodies against osteocalcin (**C)** and perilipin (**D**) of subcutaneous tissue. The arrows indicate subcutaneous tissue and generated bone, and the bars indicate bone densities. Scale bars, 100 μm. (**E-F**) Around 2 mm diameter of calvarial defect was implanted with hydrogel alone served as controls (Ctrl) or a mixture of hydrogel and 1×10^6 of normal adipocytes (nADs) or adipocytes exposed to myeloma cells ARP-1 or RPMI8226. Shown are the representative μ-CT images of calvarial defect areas (**E**). The new bone formation was highlighted in green. Scale bars, 1 mm. Semiquantitative analysis showing the relative amount of new bone formation

in the calvarial defect area from groups described in d (**F**). Representative results of three experiments are shown. $^{**}P < 0.01$. All *P* values were determined using one way ANOVA.

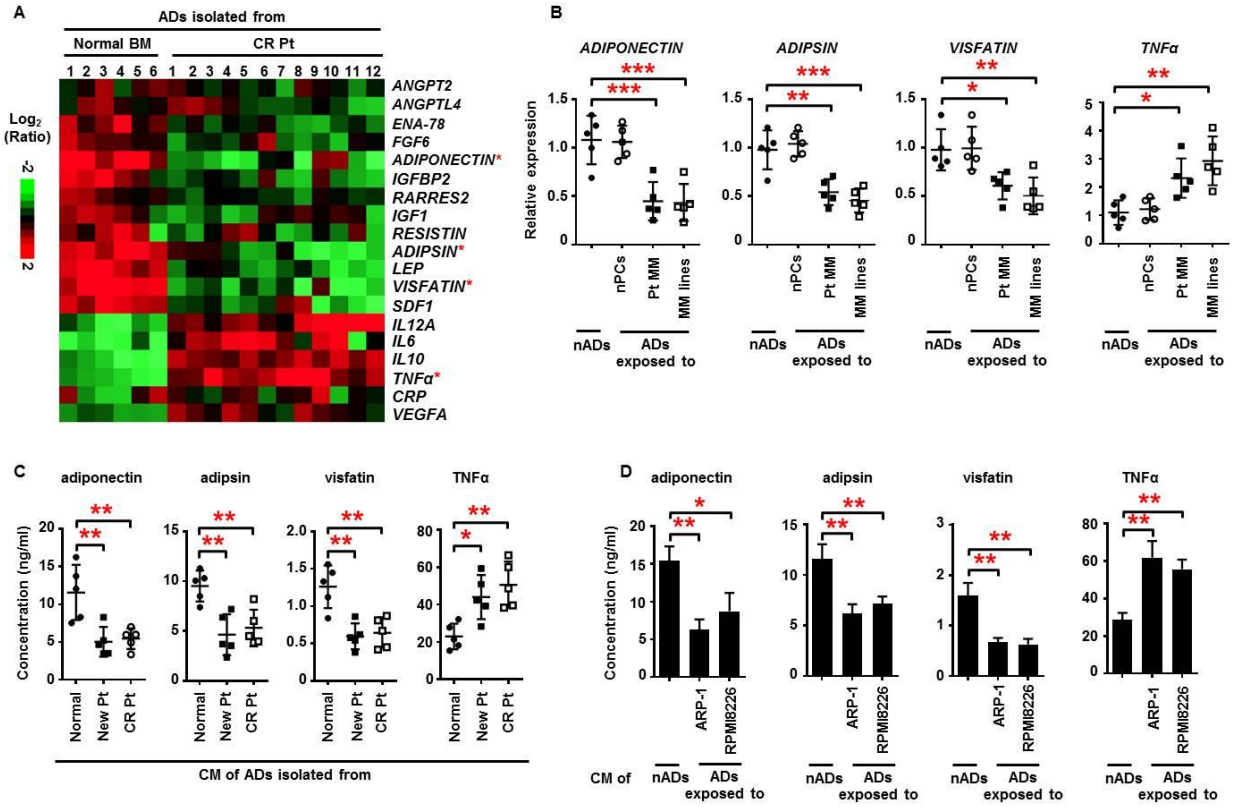

Fig. S6. Expression of adipokines in myeloma-associated adipocytes. (**A**) Heat map of the expression profile of adipokine genes in adipocytes (ADs) isolated from normal BM samples (n = 6) and the marrow of patients in complete remission (CR Pt; n = 12). (**B**) The relative expression of *ADIPONECTIN*, *ADIPSIN*, *VISFATIN*, and *TNFα* in normal adipocytes (nADs) and the adipocytes exposed to normal plasma cells (nPCs; n = 5), patient-derived myeloma cells (Pt MM; n = 5), or the myeloma cell lines (MM lines: ARP-1, RPMI 8226, U266, MM.1S, and CAG). (**C-D**) ELISA analysis results demonstrating the secretion of adiponectin, adipsin, visfatin, and TNFα in culture of adipocytes isolated from normal marrow (n=5), the marrow of CR Pt (n=5) or patients with newly diagnosed myeloma (New Pt; n=5) (**C**) and in culture of nADs or adipocytes exposed to ARP-1 or RPMI8226 (**D**). Data are averages ± SD. Each experiment was repeated three times. *P < 0.05; **P < 0.01; ***P < 0.001. All P values were determined using one way ANOVA.

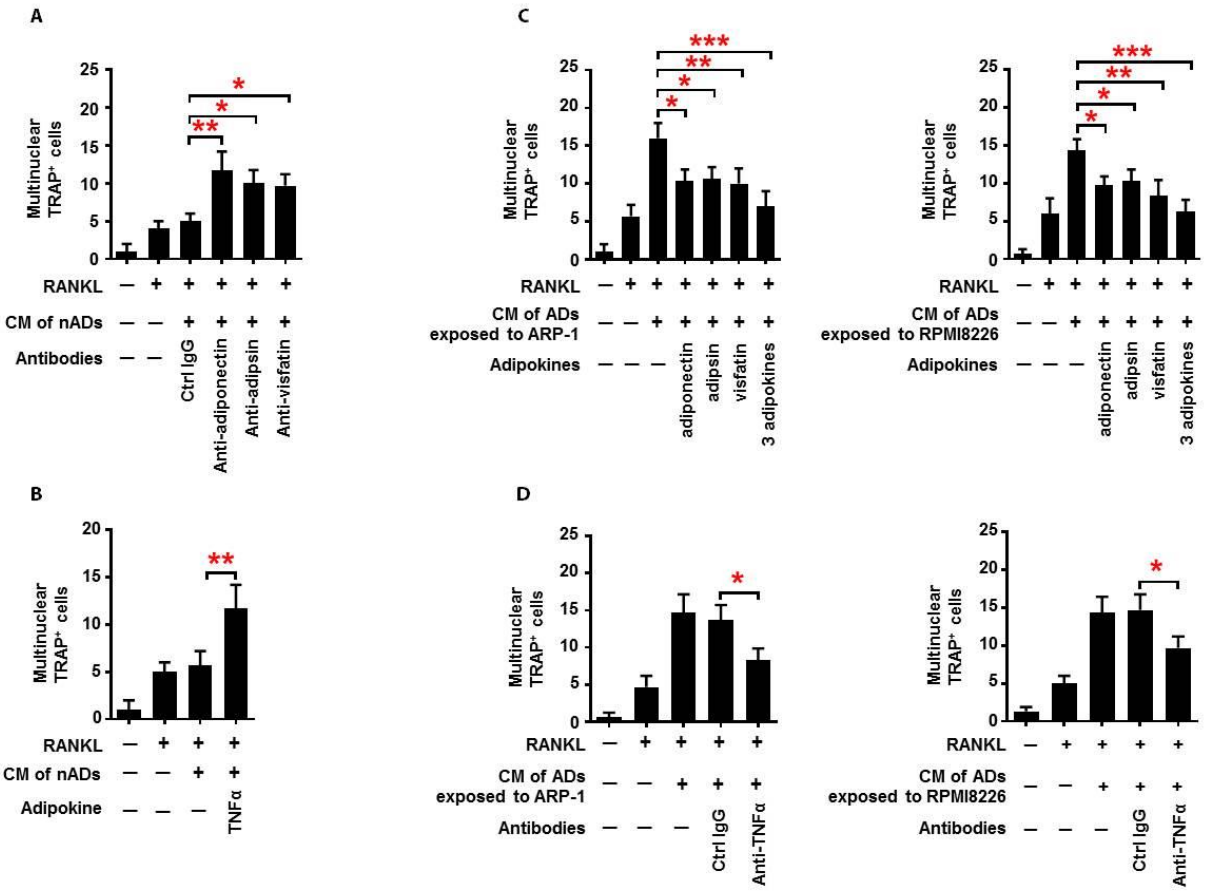

Fig. S7. Adipokines secreted from myeloma-associated adipocytes enhance osteoclast differentiation. (**A-B**) The numbers of multinuclear TRAP$^+$ cells among precursors of osteoclasts cultured with CM from normal adipocytes (nADs) in the presence of antibodies against adiponectin, adipsin, or visfatin (**A**) or in the presence of the adipokine TNFα (**B**). (**C-D**) The numbers of multinuclear TRAP$^+$ cells among precursors cultured with CM from adipocytes (ADs) exposed to ARP-1 (left) or RPMI8226 (right) cells in the presence of recombinant adiponectin (10 μg/ml), adipsin (4 μg/ml), or visfatin (10 ng/ml) alone or a combination of all three adipokines (**C**) or in the presence of an anti-TNFα antibody (**D**). Addition of control (Ctrl) IgG served as controls. Data are averages ± SD. Each experiment was repeated three times. *$P < 0.05$; **$P < 0.01$; ***$P < 0.001$. All P values were determined using one way ANOVA.

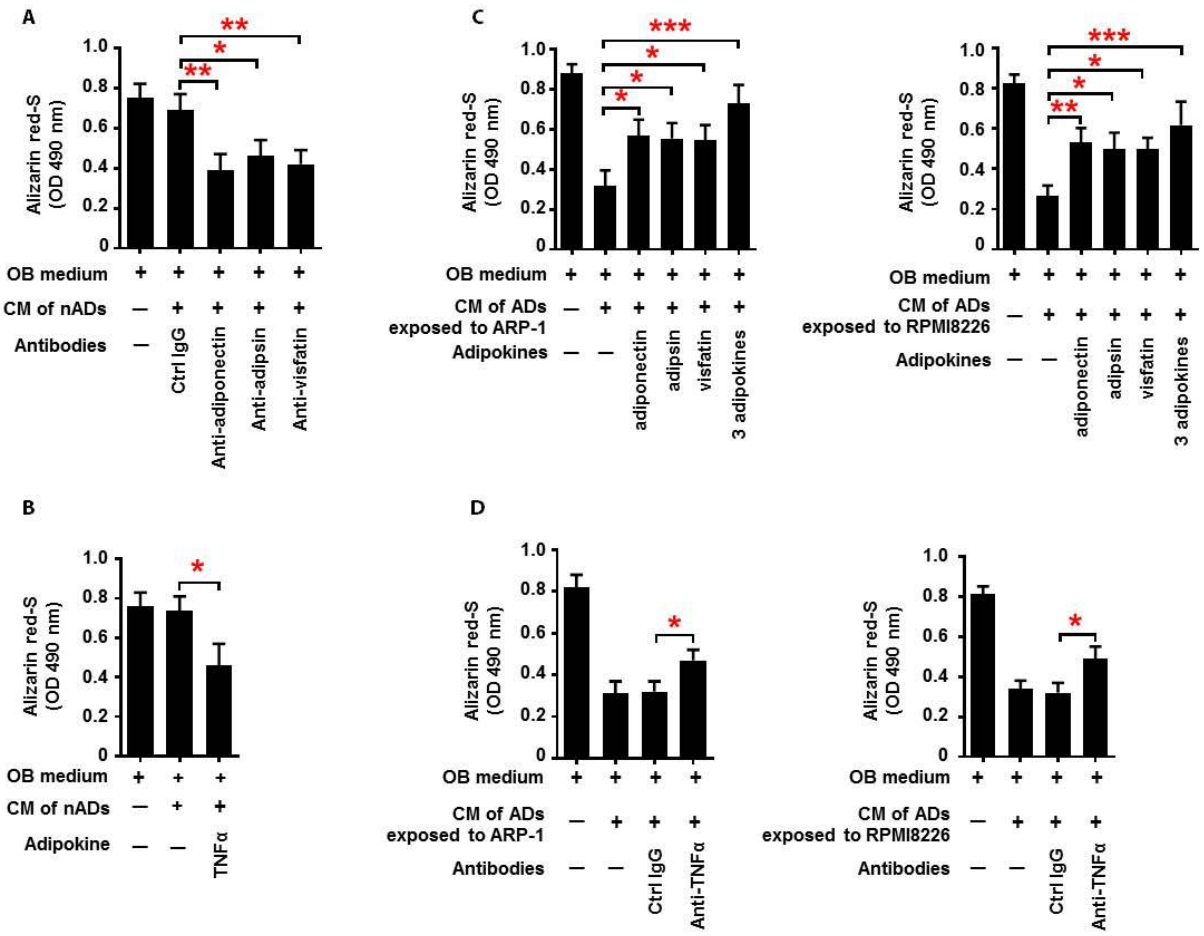

Fig. S8. Adipokines secreted from myeloma-associated adipocytes suppress osteoblast differentiation. (**A-B**) The Alizarin red S staining of MSCs cultured in osteoblast (OB) medium with CM from normal adipocytes (nADs) in the presence of antibodies against adiponectin, adipsin, or visfatin (**A**) or in the presence of the adipokine TNFα (**B**). (**C-D**) The Alizarin red S staining of MSCs cultured with CM from adipocytes (ADs) exposed to ARP-1 (left panel) or RPMI8226 (right panel) cells in the presence of recombinant adiponectin (10 μg/ml), adipsin (4 μg/ml), or visfatin (10 ng/ml) alone or a combination of all three adipokines (**C**) or in the presence of an anti-TNFα antibody (**D**). Addition of control (Ctrl) IgG served as controls. Data are averages ± SD. Each experiment was repeated three times. *$P < 0.05$; **$P < 0.01$; ***$P < 0.001$. All P values were determined using one way ANOVA.

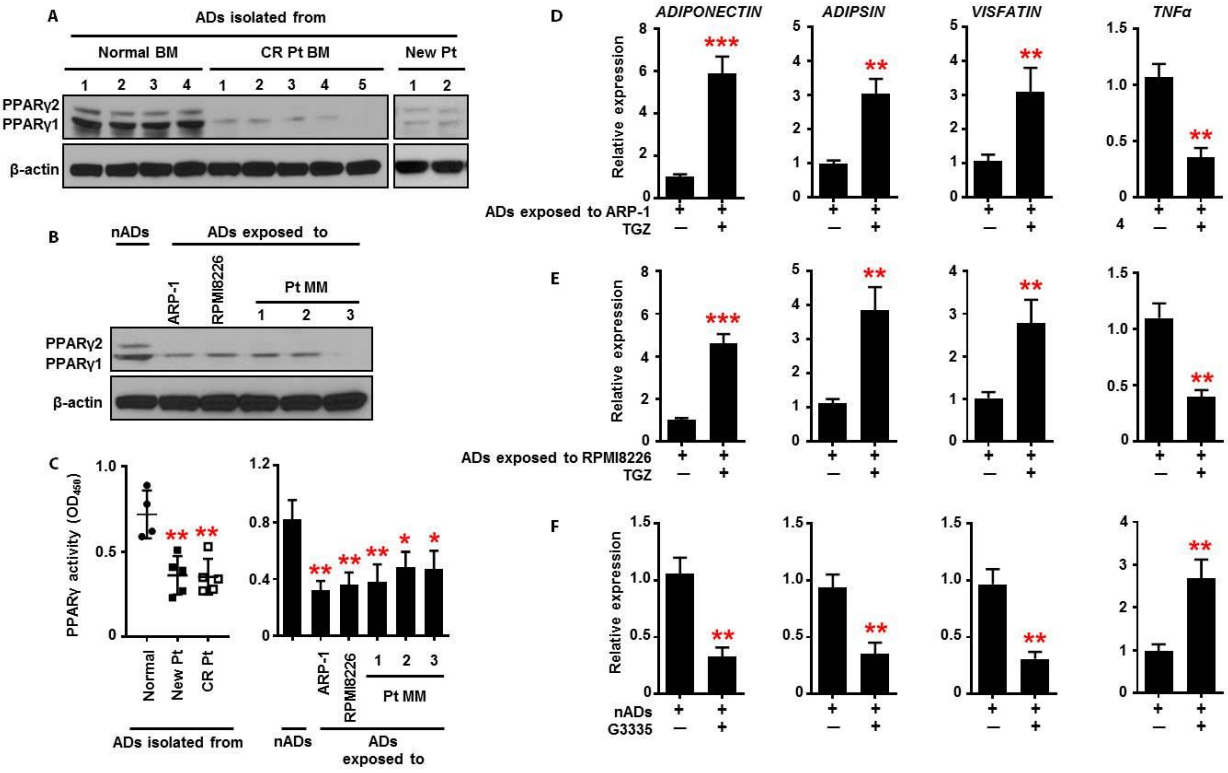

Fig. S9. Reduced expression of PPARγ in myeloma-associated adipocytes. (**A-C**) Shown are the expression (**A, B**) and activity (**C**) of PPARγ in adipocytes (ADs) isolated from normal BM samples (n=4), marrow of patients in complete remission (CR Pt; n=5), patients with newly diagnosed myeloma (New Pt; n=5) or normal adipocytes (nADs) or adipocytes exposed to ARP-1, RPMI8226, or patient-derived myeloma cells (Pt MM). (**D-F**) Real-time PCR analysis showing the relative expression of *ADIPONECTIN*, *ADIPSIN*, *VISFATIN*, and *TNFα* in adipocytes exposed to ARP-1 (**D**) or RPMI8226 (**E**) cells cultured with the PPARγ agonist troglitazone (TGZ; 5 μM) and nADs cultured with the PPARγ antagonist G3335 (10 μM) (**F**). Data are averages ± SD. Each experiment was repeated three times. **P* < 0.05; ***P* < 0.01; ****P* < 0.001. *P* values were determined using the Student *t*-test for comparison of two groups, and one way ANOVA for comparison of multiple groups.

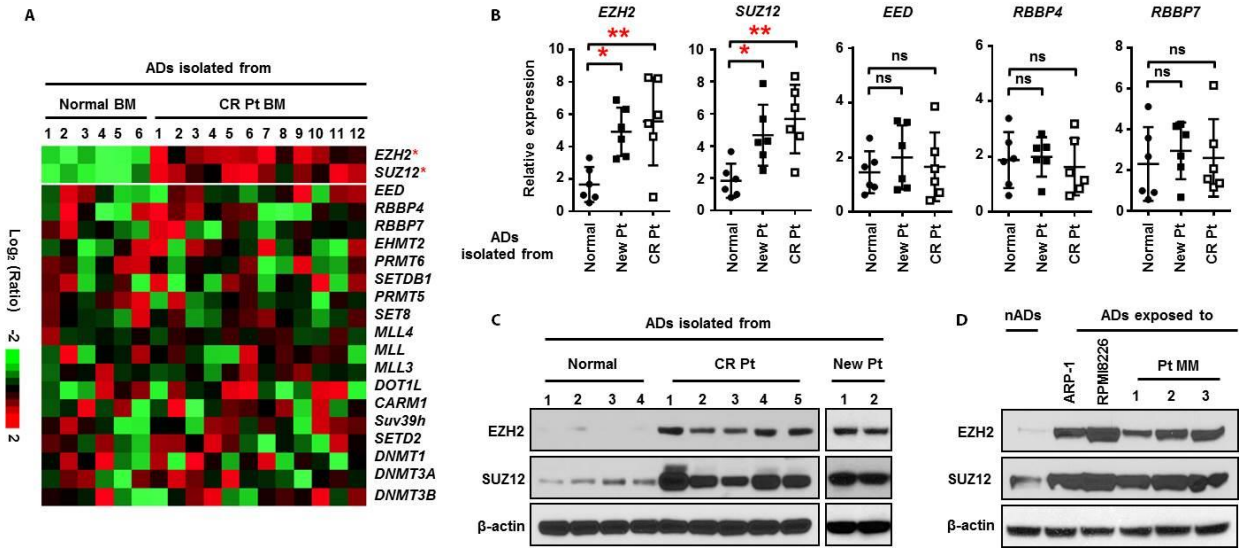

Fig. S10. Elevated expression of the PRC2 proteins EZH2 and SUZ12 in myeloma-associated adipocytes. (**A**) Heat map showing the expression profile of genes encoding for the enzymes that regulate DNA and histone methylation in adipocytes isolated from normal BM samples (*n* = 6) or BM from patients in complete remission (CR Pt; *n* = 12). (**B**) Real-time PCR analysis showing the relative expression of *EZH2*, S*UZ12*, *embryonic ectoderm development* (*EED)*, and *RB binding protein (RBBP)4/7* in adipocytes (ADs) isolated from normal (*n* = 6), CR Pt (*n* = 6), newly diagnosed patient (New Pt; *n* = 6) BM samples. (**C-D**) Western blots showing the expression of EZH2 and SUZ12 protein in adipocytes isolated from normal (*n* = 4), CR Pt (*n* = 5), or New Pt (*n* = 2) BM (**C**) nADs and adipocytes exposed to ARP-1, RPMI8226 cells, or patient-derived myeloma cells (Pt MM; *n* = 3) (**D**). Data are averages ± SD. Each experiment was repeated three times. ns, not significant. **P* < 0.05; ***P* < 0.01. All *P* values were determined using one way ANOVA.

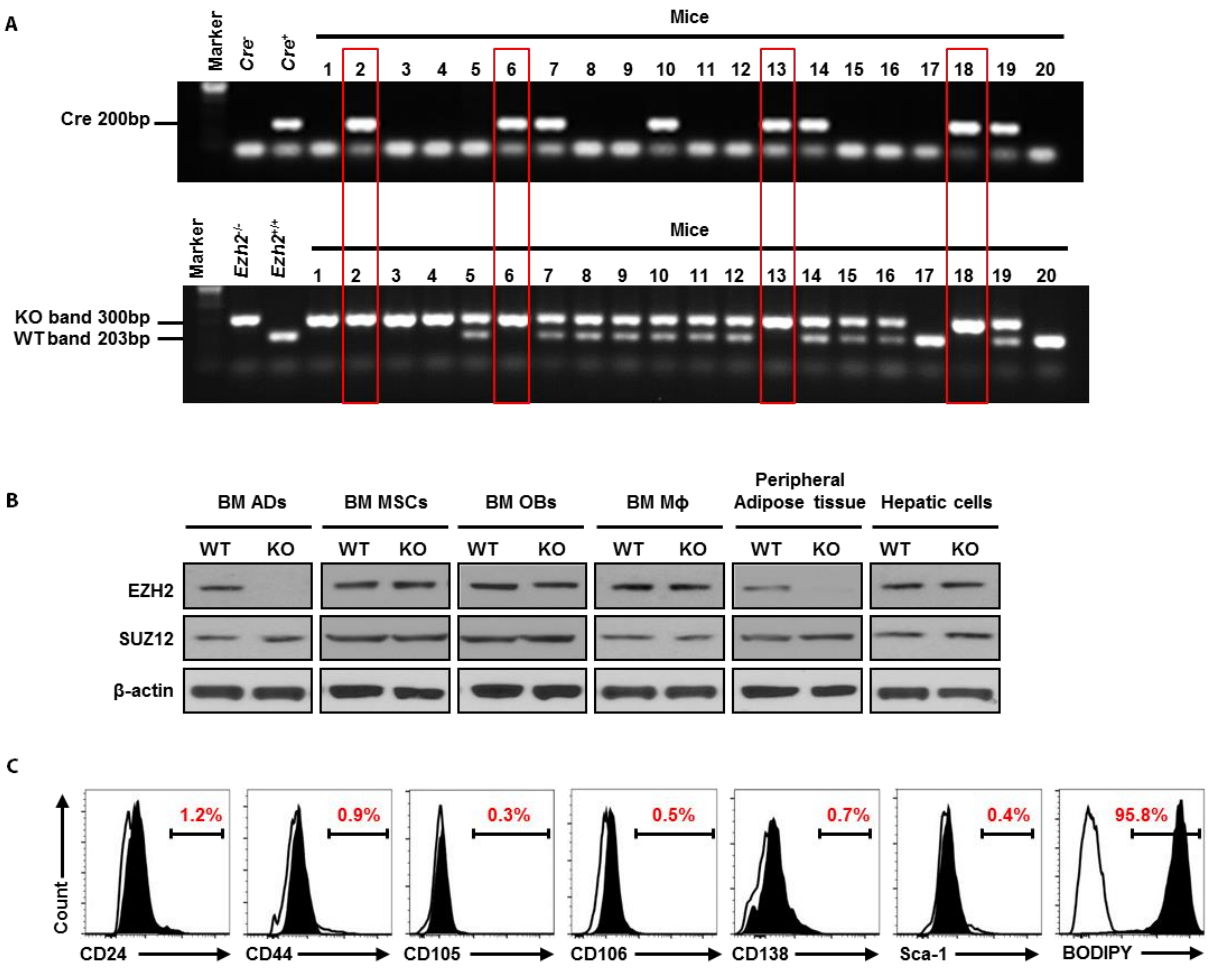

Fig. S11. Characterization of adipocyte-targeted *Ezh2*-knockout mice. (**A**) *Ezh2*-knockout (KO) genotyping using PCR. *Ezh2*-floxed mice were crossed with *Cre* mice to generate Cre-expressing *Ezh2*-KO mice. Using specific genomic DNA primers recommended by The Jackson Laboratory, the *Cre* locus was recognized as shown in the upper panel, and wild-type (WT) and KO genotypes were recognized according to their distinctive sizes (lower panel). The Cre-expressing *Ezh2*-KO mice are boxed in red. (**B**) Western blots showing the expression of EZH2 and SUZ12 in BM adipocytes (ADs), MSCs, osteoblasts (OBs), macrophages (MΦ), and peripheral adipose tissue or hepatic cells of WT and KO mice. The expressions of β-actin served as loading controls. (**C**) Characterization of mouse adipocytes isolated from mice by flow cytometry. Shown are representative histograms of CD24, CD44,

CD105, CD106, CD138, Sca-1, and BODIPY in the adipocytes. Data are representative of triplicate blots.

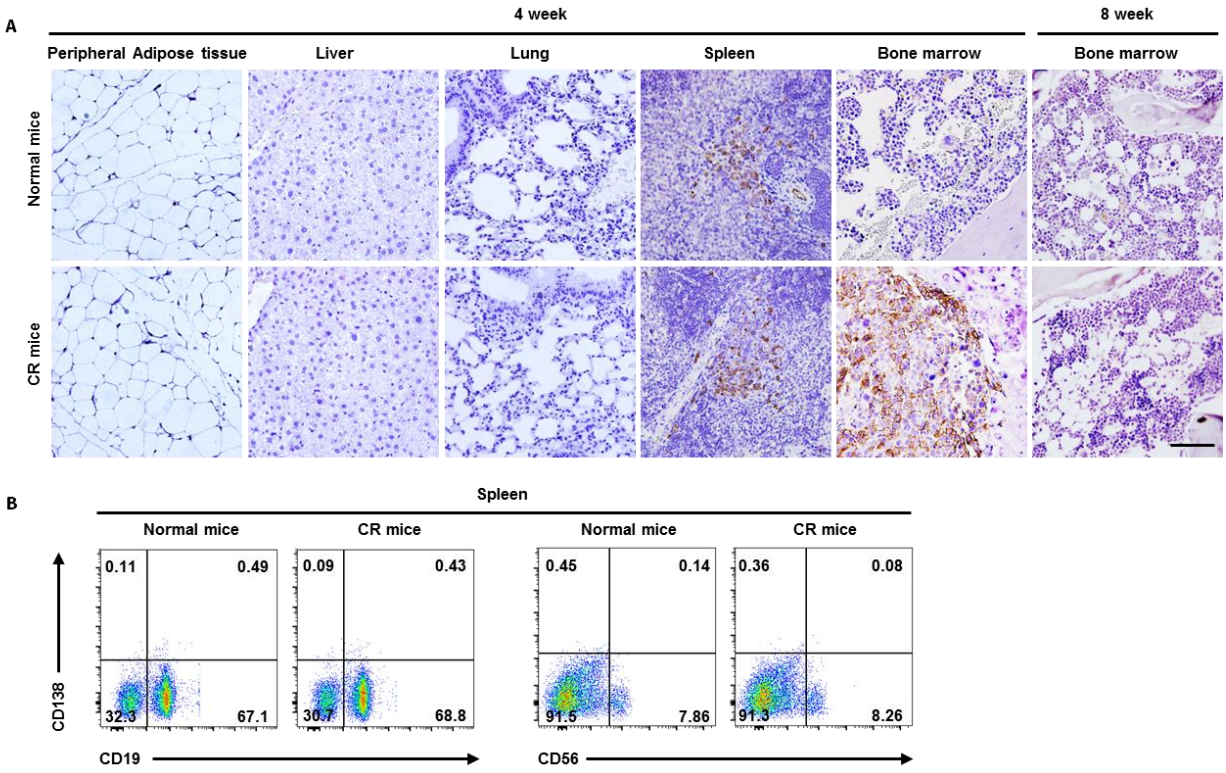

Fig. S12. Distribution of myeloma cells in the Vk*MYC myeloma cell–bearing mice. Wild-type mice were intrafemorally injected with Vk*MYC myeloma cells (1×10^6 cells/mouse) or PBS without myeloma cells (normal mice). After 4 weeks, mice were treated with chemo drugs and were in complete remission from week 6 (CR mice). The tissues were stained with an anti-CD138 antibody for immunohistochemistry, and the spleen cells were analyzed with flow cytometry labeled with the antibody against CD138, CD19, or CD56. (**A**) Shown are $CD138^+$ cells in peripheral adipose tissue, live, lung, spleen, and BM of mice before chemotherapy (4 week) or in the BM after chemotherapy (8 week). (**B**) Characterization of normal plasma cells in murine spleen. The cells were stained with surface markers for the plasma and myeloma cells, and examined by flow cytometry. Scale bars, 100 μm. Representative results of three experiments are shown.

Table S1. Identification of SP1 that binds to the PRC2 complex in adipocytes using mass spectrometry.

Gene name	Peptide
EZH2	R.IGIFAKR.A
	R.YSQADALK.Y
	K.EFAAALTAER.I
	R.TEILNQEWK.Q
	R.IKTPPKRPGGR.R
	R.FANHSVNPNCYAK.V
	R.IQPVHILTSVSSLR.G
	R.AIQTGEELFFDYR.Y
	R.RIQPVHILTSVSSLR.G
	K.RAIQTGEELFFDYR.Y
	R.VLIGTYYDNFCAIAR.L
	K.ESSIIAPAPAEDVDTPPR.K
	R.ECSVTSDLDFPTQVIPLK.T
	R.VKESSIIAPAPAEDVDTPPR.K
	R.GTRECSVTSDLDFPTQVIPLK.T
	K.IFEAISSMFPDKGTAEELKEK.Y
	K.MKPNIEPPENVEWSGAEASMFR.V
SUZ12	R.QVPTGKK.Q
	R.VTRPGRR.E
	R.KLYSLLK.H
	K.SYSLLFR.V

	R.QPGFAFSR.N
	K.LREMQQK.L
	R.TLTYMSHR.N
	K.LWNLHVMK.H
	R.ATWETILDGK.R
	K.ESLTTDLQTR.K
	K.ALETDSVSGVSK.Q
	K.STAPIAKPLATR.N
	K.TFVAQMTVFDK.N
	R.TPITHILVCRPK.R
	K.EKALETDSVSGVSK.Q
	K.ASMSEFLESEDGEVEQQR.T
	R.LPPFETFSQGPTLQFTLR.W
	K.ASMSEFLESEDGEVEQQR.T
	R.NREDGEKTFVAQMTVFDK.N
SP1	K.FACPECPKR.F
	R.FTRSDELQR.H
	K.DSEGRGSGDPGK.K
	K.KQHICHIQGCGK.V
	K.GGPGVALSVGTLPLDSGAGSEGSGTATPSA LITTNMVAMEAICPEGIAR.L
	R.VSGLQGSDALNIQQNQTSGGSLQAGQQK.E
EED	K.IHFPDFSTR.D
	K.ESYDYNPNK.T

	K.MLALGNQVGK.L
	K.IKPSESNVTILGR.F
	R.EVSTAPAGTDMPAAK.K
	R.FSMDFWQKMLALGNQVGK.L
	K.MEDDIDKIKPSESNVTILGR.F
	K.CVNSLKEDHNQPLFGVQFNWHSK.E
RBBP7	K.TVALWDLR.N
	R.LNVWDLSK.I
	K.INHEGEVNR.A
	K.TPSSDVLVFDYTK.H
	K.IGEEQSPEDAEDGPPELLFIHGGHTAK.I
RBBP4	R.RLNVWDLSK.I
	K.IGEEQSAEDAEDGPPELLFIHGGHTAK.I

Table S2. Characteristics of patients with myeloma and donors with normal BM.

Patient	Age (year)	Gender	BMI	Treatment
1	67	M	37.7	RTx/Cfz/Len/Dex
2	59	F	33.06	Btz/Dex/Len/Mel/Elo/Dara
3	62	M	24.9	Cfz/Len/Dex/Mel/Elo
4	66	F	19	Cfz/Len/Dex/Mel
5	66	M	26.4	Len/Btz/Dex/Pano/Cfz/RTx/Elo
6	64	M	29	Cy/Btz/Dox/Dex/RTx/Cfz/Poma/Len/Ixa
7	51	M	21.29	Btz/Cy/Dex/Len/Mel/Cfz/Poma
8	64	M	27.1	Cfz/Cy/Dex/RTx/Mel/Len
9	58	F	20.8	Len/Btz/Dex/Cfz/Mel/Poma/Elo/Ixa
10	51	M	25.8	Len/Btz/Dex/Mel
11	76	M	33.5	Cfz/Len/Dex/Mel/Dara/Btz
12	72	F	22.9	Btz/Len/Dex/RTx/Elo/Cfz/Poma
13	69	F	22.5	Btz/Len/Dex/RTx/Mel
14	41	M	30.2	Btz/Len/Dex/RTx/Mel/Cfz
15	72	F	25	Btz/Dex
16	59	M	28.7	Btz/Dex/Cy
17	71	F	28.9	Btz/Dex
18	60	F	26.7	Btz/Dex/Cy
19	76	M	25.6	Btz/Dex
20	72	F	24.9	Btz/Dex
21	71	F	26.4	Tha/Mel/Len/Dex/Btz
22	46	F	30.8	Dex/Len/Tha
23	71	M	24.4	Btz/Dex/Dox/Len
24	42	F	33.8	Btz/Dex/Dex/Len/Cy/Mel/BU
25	51	M	30.3	Dex/Btz/Cy/Len
26	49	M	31.3	Btz/Tha/Dex/Len/Cy
27	76	M	28.7	RTx/Cy/Vin/Dox/Dex/Btz

Abbreviations: Len: Lenalidomide; Btz: bortezomib; Dex: Dexamethasone; Ixa: Ixazomib; Cfz: Carfilzomib; Mel: Melphalan; RTx: Radiation Therapy; Tha: thalidomide; Pem: Pembrolizumab; Poma: Pomalidomide; Vin: vincristine; BU: Busulfan; Cy: cyclophosphamide; PAN: Panobinostat; ELO: Elotuzumab; Dox: doxorubicin; Dara: Daratumumab.

Normal BM	Age (year)	Gender	BMI
1	46	F	29.1
2	55	F	38.9
3	68	F	44.4
4	47	M	26.2
5	52	F	19.5
6	59	M	31.1
7	68	M	31.4
8	64	M	29.1
9	74	F	22.7
10	47	M	24.1
11	66	M	30.6

Table S3. Primers used in real-time reverse transcription PCR analysis.

Gene	Forward	Reverse
GAPDH	CTGGGCTACACTGAGCACC	AAGTGGTCGTTGAGGGCAATG
TRAP	AGATCCTGGGTGCAGACTTC	AAGGGAGCGGTCAGAGAATA
CALCR	GGGAATCCAGTTTGTCGTCT	ACAAAGAAGCCCTGGAAATG
CTSK	CCATATGTGGGACAGGAAGA	CCTCTTCAGGGCTTTCTCAT
BGLAP	ACTGTGACGAGTTGGCTGAC	AAGAGGAAAGAAGGGTGCCT
ALP	TCCCAGTTGAGGAGGAGAAC	CCCAGGAAGATGATGAGGTT
COL1A1	TGTTCAGCTTTGTGGACCTC	GGTGATTGGTGGGATGTCTT
ANGPT2	AACTTTCGGAAGAGCATGGAC	CGAGTCATCGTATTCGAGCGG
ANGPTL4	GGCTCAGTGGACTTCAACCG	CCGTGATGCTATGCACCTTCT
ENA-78	AGCTGCGTTGCGTTTGTTTAC	TGGCGAACACTTGCAGATTAC
FGF6	GGAAGATTGTACGCAACGCC	GGCATTGTAATTGTTGGGCAG
ADIPONECTIN	AACATGCCCATTCGCTTTACC	TAGGCAAAGTAGTACAGCCCA
IGFBP2	GACAATGGCGATGACCACTCA	CAGCTCCTTCATACCCGACTT
CHEMERIN	AGAAACCCGAGTGCAAAGTCA	AGAACTTGGGTCTCTATGGGG
IGF1	GCTCTTCAGTTCGTGTGTGGA	GCCTCCTTAGATCACAGCTCC
RESISTIN	CTGTTGGTGTCTAGCAAGACC	CCAATGCTGCTTATTGCCCTAAA
ADIPSIN	GACACCATCGACCACGACC	GCCACGTCGCAGAGAGTTC
LEP	TGCCTTCCAGAAACGTGATCC	CTCTGTGGAGTAGCCTGAAGC
VISFATIN	AATGTTCTCTTCACGGTGGAAAA	ACTGTGATTGGATACCAGGACT
SDF1	ATTCTCAACACTCCAAACTGTGC	ACTTTAGCTTCGGGTCAATGC
TNFα	GAGGCCAAGCCCTGGTATG	CGGGCCGATTGATCTCAGC
PPARγ	ACCAAAGTGCAATCAAAGTGGA	ATGAGGGAGTTGGAAGGCTCT

EZH2	GGACCACAGTGTTACCAGCAT	GTGGGGTCTTTATCCGCTCAG
SUZ12	AGGCTGACCACGAGCTTTTC	GGTGCTATGAGATTCCGAGTTC
EED	GTGACGAGAACAGCAATCCAG	TATCAGGGCGTTCAGTGTTTG
RBBP4	CAGCATTCATCGACTTGTCCT	TGTGACGCATCAAACTGAGCA
RBBP7	GAGGAGCGTGTCATCAATGAA	GCATGGGTCATAACCAGGTCATA
Gapdh	CCTCCTGCAGACAGACGTAA	AGCATCGACCAGTGCTACAG
Ezh2	AGTGACTTGGATTTTCCAGCAC	AATTCTGTTGTAAGGGCGACC
Suz12	AACTCGAAATCTTATCGCACCAA	TGCAAATGTGCAGACAAGCTAT
Pparγ	TCGCTGATGCACTGCCTATG	GAGAGGTCCACAGAGCTGATT
Adiponectin	TGTTCCTCTTAATCCTGCCCA	CCAACCTGCACAAGTTCCCTT
Adipsin	CATGCTCGGCCCTACATGG	CACAGAGTCGTCATCCGTCAC
Visfatin	GCAGAAGCCGAGTTCAACATC	TTTTCACGGCATTCAAAGTAGGA
Tnfα	CCCTCACACTCAGATCATCTTCT	GCTACGACGTGGGCTACAG

Table S4. Primers used in ChIP-PCR.

PPARγ promoter subregion	Forward	Reverse
R1	AAAAGCAGGCTAGGCGCAGT	ACTGTGTCTTGACATGTTGCCT
R2	CCCAAAGAGGATCAGGCCCA	TTCCTGCCACGCTGTCCATC
R3	GTGGCGAGGAGCAAACGACA	GCGACTGGGAGGGAGCGG
R4	CGGGGGAACTTTGGAGCAGG	CTCTGGACAGCGAACGGGAC